

## Low Frequency Magnetolectric Sensor Without Bias Using Laminated Metglas/Quartz/Metglas Structure

© Changxing Sun<sup>1</sup>, Wenrong Yang<sup>1,¶</sup>, Yifan He<sup>2</sup>, Lei Chen<sup>2</sup>, Cunzheng Dong<sup>2</sup>, Xianfeng Liang<sup>2</sup>, Huaihao Chen<sup>2</sup>, Nian-Xiang Sun<sup>2</sup>

<sup>1</sup> State Key Laboratory of Reliability and Intelligence of Electrical Equipment, Hebei University of Technology, Tianjin, China

<sup>2</sup> Department of Electrical and Computer Engineering, Northeastern University, Boston, Massachusetts, USA

¶ E-mail: wryang@hebut.edu.cn

Received April 7, 2021

Revised June 11, 2021

Accepted June 13, 2021

Tremendous progress has been made on boosting the performance of magnetolectric sensor to detect low frequency magnetic field signal by frequency multiplication based on magnetolectric composites. In this paper, a novel magnetolectric sensor based on the laminated Metglas/piezoelectric quartz crystal/Metglas composites structure is presented. The Metglas foils are bonded symmetrically on both sides of the X-cut quartz crystal plate with epoxy. Experiments showed that the ME composites sensor was able to achieved a limit of detection of 11 pT for a low frequency magnetic field 1 Hz without any bias field through frequency multiplication method. The noise power spectrum density of the sensor has also been tested to be  $3.93 \cdot 10^{-6} \text{ V/Hz}^{1/2}$  at 1 Hz. The results indicate that the proposed sensor has favorable features, which provides a cost-effective and high-performance approach for low frequency magnetic field measurement.

**Keywords:** Low frequency, limit of detection, magnetolectric sensor, piezoelectric quartz crystal.

DOI: 10.21883/TPL.2022.13.53347.18814

Magnetolectric (ME) materials have been extensively studied in recent years and are of interest because of their wide range of applications: magnetolectric sensors, mechanical antennas, storage and tunable microwave devices, etc. [1–4]. ME composites made of piezoelectric and magnetostrictive materials can provide higher ME voltages than complex single-phase multiferroic materials. Various types of composite materials, such as powder-filled or layered composites, have also been proposed to achieve high efficiency of ME heterostructures, which are used in different modes of vibration. The application area of powder-filled magnetolectric composites is limited due to their relatively weak mechanical coupling, low ME coefficient and high dielectric losses [5]. In contrast, layered ME composites have a higher ME coefficient and a simpler structure, which greatly simplifies the manufacturing process. On the structure of PMN–PT monocrystalline fiber laminated with laser-irradiated amorphous FeBSi alloy using epoxy adhesive, high magnetolectric coefficient can be obtained at resonance frequency at low temperatures, reaching  $7000 \text{ V}/(\text{cm} \cdot \text{Oe})$  [6]. Triple-layer laminated ME sensors have a high ME coefficient at the resonance frequency in the kilohertz range, while two-layer ME sensor structures with a resonance frequency of bending oscillations of several hundred Hz [7] are proposed for recording magnetic fields of lower frequency.

However, recording biomagnetic signals in the picoTesla range or lower at low frequencies from 1 to 100 Hz is always a very difficult task because of the high level of noise proportional to  $1/f$ . Highly sensitive superconducting quantum interferometric detectors (SQUID) are

currently used to record low-frequency biomagnetic signals at extremely low operating temperatures. A promising alternative to SQUID in the area of biomagnetic signal registration are highly sensitive and compact ME sensors [8]. To be able to enhance the magnetolectric effect of the layered ME sensor, its piezoelectric phase must have a high piezoelectric coefficient and low dielectric permittivity. Compared to piezoelectric transducers, monocrystalline piezoelectric quartz has more favorable properties, its piezoelectric modulus to dielectric permittivity ratio being  $0.05 \text{ m}^2/\text{C}$  [9,10]. Besides, the high quality factor of quartz-based devices ensures the absence of ferroelectric hysteresis and pyroelectric loss effects.

This paper proposes an innovative magnetolectric sensor with a three-layer structure consisting of a quartz crystal cut perpendicular to the X axis and Metglas foil. The low-frequency magnetic field signal is generated and detected by a quartz sensor using a frequency modulation circuit. The sensitivity limit of the ME sensor was determined in the absence of DC bias.

In the manufacture of the sensor, a quartz plate  $500 \mu\text{m}$  thick, cut perpendicular to the X axis and polished on both sides, was cut into plates of  $72 \times 9 \text{ mm}$  size. Thin (100 nm) platinum films were applied to both sides of the plate by magnetron sputtering as electrodes. The  $21 \mu\text{m}$  thick amorphous metal Metglas foil films with high magnetostrictive capacity were cut into  $70 \times 9 \text{ mm}$  pieces. Ten layers of Metglas foil were stacked on top of each other and glued symmetrically with epoxy adhesive on both sides of the quartz plate. Metglas layers were aligned along the edge of one long side of the quartz plate. Finally,

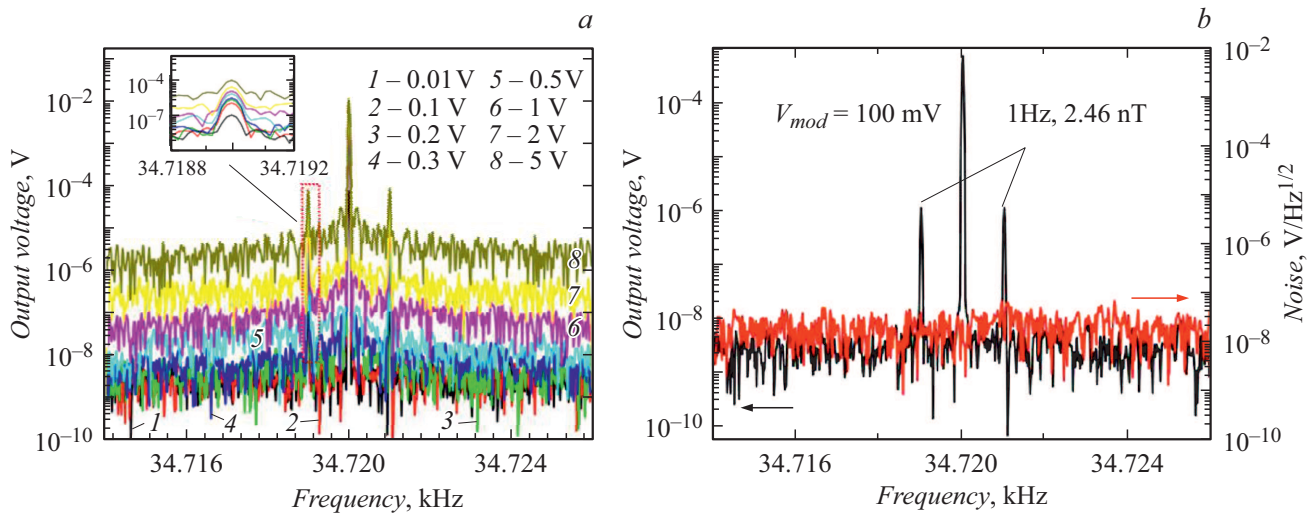


**Figure 1.** Measurement data of modulating spectrum and noise signal. *a* is the voltage dependence of the induced voltage of the ME sensor at different modulating voltages. *b* is the output voltage and noise signal spectrum.

the Metglas/quartz/Metglas layered structure was vacuum packed and incubated for 24 h at room temperature in order to minimize the thickness of the epoxy film between the layers. The finished device was installed in a homemade modulation coil for low-frequency measurements.

In this case, due to the high noise power density and low ME coefficient in the low-frequency range, it was necessary to use frequency conversion to register low-frequency magnetic field, less than 100 pT strong. In case such scheme is adopted, the modulated frequency component gets generated near the region of resonance, and the intensity of the component is proportional to the intensity of the registered low-frequency magnetic signal. If a low strength magnetic field  $H$  is applied to the ME sensor, the coefficient of direct ME interaction  $\alpha_{ME}$  is given by the formula  $\alpha_{ME} = \partial V_{ME} / \partial H$ . The value  $V_{ME}$  represents the voltage induced in the piezoelectric phase to which the deformation stress of the magnetostrictive Metglas layers is transferred. Magnetostrictive response of the amorphous Metglas tape can be described using the Livingston model for coherent magnetization rotation. Within the frame of the Livingston model [11], the strain stress of the magnetostrictive material is described by the formula  $S = CH^2$ . Here  $H$  is the applied magnetic field strength,  $C$  is the magnetostrictive parameter. In case the total magnetic field applied to the sensor can be represented as  $H = H_{mod}(t) + H_{sig}(t)$ , then the deformation of magnetostrictive material is described by the formula

$$S = C(H_{sig}(t)^2 + 2H_{sig}(t)H_{mod}(t) + H_{mod}(t)^2), \quad (1)$$

where  $H_{mod}$  is the modulating signal, and  $H_{sig}$  is the detectable weak AC signal. If the magnetically modulated sensor output signal is processed by a band-pass filter or a synchronizing amplifier, its formula takes the following form:

$$S = 2CH_{sig}(t)H_{mod}(t).$$

If

$$H_{sig}(t) = H_{sig} \cos(2\pi f_{sig}t)$$

and

$$H_{mod}(t) = H_{mod} \cos(2\pi f_{mod}t),$$

the deformation is described as follows:

$$\begin{aligned} 2H_{sig}(t)H_{mod}(t) &= 2H_{mod}H_{sig} \cos(2\pi f_{mod}t) \cos(2\pi f_{sig}t) \\ &= H_{mod}H_{sig} \cos(2\pi(f_{mod} + f_{sig})t) \\ &\quad + H_{mod}H_{sig} \cos(2\pi(f_{mod} - f_{sig})t), \quad (2) \end{aligned}$$

where  $f_{mod}$  and  $f_{sig}$  are the frequencies of the modulating signal and the weak AC signal, respectively. For modulating frequency  $f_{mod}$ , the resonant frequency of the sensor is selected, which ensures its high sensitivity in the low-frequency mode.

The sensor is placed in the center of a pair of Helmholtz coils. Helmholtz coils create a low-frequency magnetic signal. A homemade coil wound on the sensor plays the role of a modulating signal source. A Stanford Research Systems SR785 signal analyzer is used to measure the output signal. To eliminate electromagnetic interference, which could hinder the registration of low-frequency magnetic fields, the test setup was placed in a cylindrical chamber shielding the magnetic field.

Composite ME sensors require an external magnetic bias field to amplify the magnetoelectric effect, which increases their size and cost. In the present work, tests of the quartz sensor with magnetized amorphous metal Metglas were carried out in the absence of magnetic DC bias. The resonant frequency of the sensor was measured with an Agilent 4194A impedance analyzer and was found to be 34.72 kHz. Therefore, in order to be able to register a low-frequency (1 Hz) magnetic field, a carrier field of 34.72 kHz

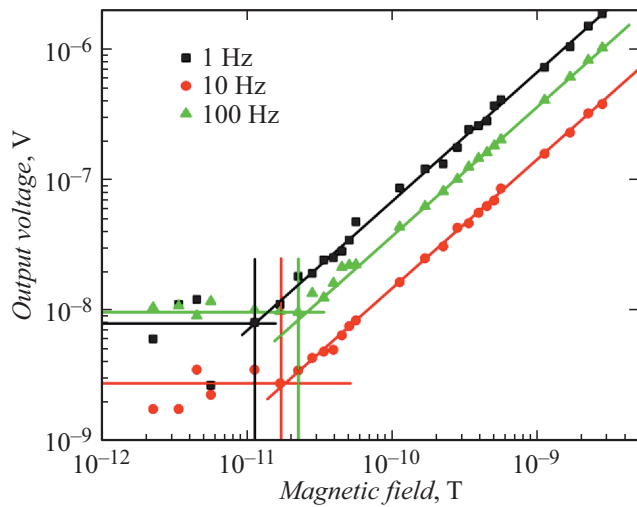


**Figure 2.** Sensitivity limit of the sensor for different frequencies.

was applied to the composite ME sensors. The output voltage spectra of the ME sensor are shown in Fig. 1.

Fig. 1, *a* shows the output voltage spectra of the ME sensor under different AC modulating fields. The spectrum contains three peaks: one is corresponding to the modulation frequency  $f_{mod}$ , and two peaks of equal amplitude on each side of it are  $f_{mod} \pm f_{sig}$ . In the inset to Fig. 1, *a*, a side peak located on the lower frequency side is shown in more detail. The induced voltage at 34.721 kHz increases as the applied modulating voltage increases. Unfortunately, noise intensity follows the same law as the induced voltage. In order to optimize the signal-to-noise ratio,  $V_{mod} = 100$  mV was chosen, corresponding to the modulating magnetic field strength  $H_{mod} = 2$  Oe. Fig. 1, *b* shows the output voltage spectrum of the ME sensor recording the magnetic field at frequency 1 Hz and induction 2.46 nT, with optimized modulating voltage amplitude and noise power spectral density in the region of resonance frequency. The peak induced voltage of the low-frequency sideband is  $1.06 \mu\text{V}$ , while the noise voltage level is 2.61 nV. With an AC magnetic field characterized by a value of 2.46 nT, the observed signal-to-noise ratio was 52.3 dB. Thus, the calculation of sensitivity limit yields a value of the order of 6 pT. Fig. 2 shows the dependence on the magnetic field of the real low-frequency limit of sensor sensitivity when using the method of frequency modulation.

When the value of  $H_{sig}$  decreases, first there is a linear decrease in the output voltage of the ME sensor from nanoTesla level to picoTesla level values of induction of the low-frequency AC magnetic field. Then the sensor output voltage ceases to correlate with the  $H_{sig}$  value, mainly because the AC ME signal is highly dependent on the noise voltage level. The point of intersection of the curves at which the signal-to-noise ratio equals 1, yields the sensitivity limit of the sensor. The sensitivity limit values were also measured at frequencies of 10 and 100 Hz. Fig. 2 shows that the sensitivity limits are 11, 16 and 22 pT at 1, 10 and

100 Hz, respectively. Such values of the sensitivity limit are typical for this type of classical symmetric resonant sensor structures. Sensitivity of the quartz sensor at 1 Hz is higher than at 10 and 100 Hz. This may be due to the high quality factor of quartz, which limits the resonance gain to a very narrow range of frequencies, a few Hz at most, when using the frequency modulation method. This feature is used to register picoTesla fields at low frequencies (1–100 Hz) and room temperature. Sensor noises were measured at room temperature using a frequency spectrum analyzer, with no external magnetic field applied to the sensor.

Fig. 3 shows the results of measuring the spectral noise power of the sensor in the range from 0.1 to 100 Hz. To eliminate external interference, measurements were carried out in a shielding chamber. From the figure one can see that the main component of the noise is at a frequency of 60 Hz, as well as at frequencies that are multiples of that value. It turned out that the noise density at 1 Hz is  $3.93 \cdot 10^{-6} \text{ V/Hz}^{1/2}$ . A low-frequency magnetic signal with an amplitude of 11 pT at 1 Hz can be registered using offset-free frequency conversion. Noise level of the SR780 spectrum analyzer is much lower than the measured noise level, and this difference is sufficient for there to be no effect of noise on measurement results.

Thus, the possibility of manufacturing the ME sensor with a three-layer structure can be considered proven. In this study the possibility was investigated of operating the proposed ME sensor to record low-frequency magnetic field using the frequency conversion method. Experimental results showed that when using the frequency conversion method, the sensitivity limit of the sensor to weak magnetic field is low and is 11, 16 and 22 pT at frequencies of 1, 10 and 100 Hz, respectively. In addition, the ability to operate the sensor in the absence of a biasing magnetic field enables a reduction of its size. Therefore, such sensors are very promising for measuring industrial magnetic fields, where instrumentation size and weight may play a significant role.

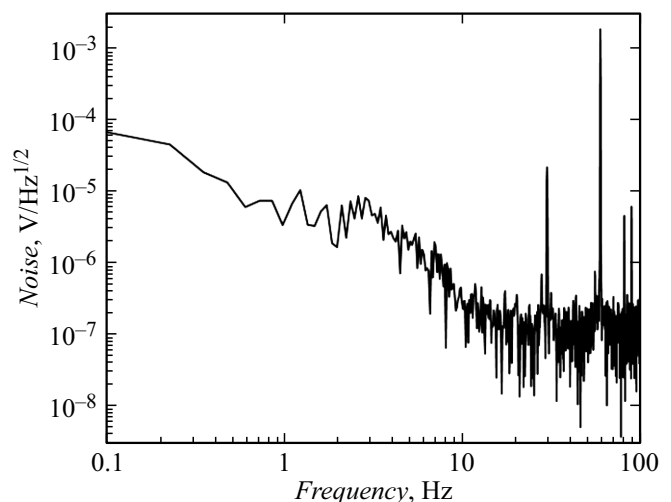


**Figure 3.** Noise spectral power measurement data of the ME sensor.

## Funding

Financial support for the study was provided by the State Key Laboratory of Reliability and Intelligence of Electrical Equipment (N EERI\_PI2020004), National Natural Science Foundation of China (51877066) and Joint Doctoral Training Foundation of HEBUT (2018HW0002).

## Conflict of interest

The authors declare that they have no conflict of interest.

## References

- [1] J. Zhai, Z. Xing, S. Dong, J. Li, D. Viehland, *J. Am. Ceram. Soc.*, **91** (2), 351 (2008).  
DOI: 10.1111/j.1551-2916.2008.02259.x
- [2] C. Dong, Y. He, M. Li, C. Tu, Z. Chu, X. Liang, H. Chen, Y. Wei, M. Zaeimbashi, X. Wang, H. Lin, Y. Gao, N.X. Sun, *IEEE Antennas Wirel. Propag. Lett.*, **19** (3), 398 (2020).  
DOI: 10.1109/LAWP.2020.2968604
- [3] V.L. Preobrazhensky, L.M. Krutyansky, N. Tiercelin, P. Pernod, *Tech. Phys. Lett.*, **46** (1), 38 (2020).  
DOI: 10.1134/S1063785020010113.
- [4] X. Liang, C. Dong, H. Chen, J. Wang, Y. Wei, M. Zaeimbashi, Y. He, A. Matyushov, C. Sun, N.X. Sun, *Sensors*, **20** (5), 1532 (2020). DOI: 10.3390/s20051532
- [5] Z. Chu, M. PourhosseiniAsl, S. Dong, *J. Phys. D: Appl. Phys.*, **51** (24), 243001 (2018). DOI: 0.1088/1361-6463/aac29b
- [6] Z. Chu, H. Shi, W. Shi, G. Liu, J. Wu, J. Yang, S. Dong, *Adv. Mater.*, **29** (19), 1606022 (2017).  
DOI: 10.1002/adma.201606022
- [7] J. Ou-Yang, X. Liu, H. Zhou, Z. Zou, Y. Yang, J. Li, Y. Zhang, B. Zhu, S. Chen, X. Yang, *J. Phys. D: Appl. Phys.*, **51** (32), 324005 (2018). DOI: 10.1088/1361-6463/aaced8
- [8] S. Zuo, J. Schmalz, M. Ozden, M. Gerken, J. Su, F. Niekkel, F. Lofink, K. Nazarpour, H. Heidari, *IEEE Trans. Biomed. Circuits Syst.*, **14** (5), 971 (2020).  
DOI: 10.1109/TBCAS.2020.2998290
- [9] V.M. Laletin, D.A. Filippov, N.N. Poddubnaya, I.N. Manicheva, G. Srinivasan, *Tech. Phys. Lett.*, **45** (5), 436 (2019).  
DOI: 10.1134/S1063785019050092.
- [10] V.M. Laletin, D.A. Filippov, S.E. Mozzharov, I.N. Manicheva, *Tech. Phys. Lett.*, **44** (4), 281 (2018).  
DOI: 10.1134/S1063785018040065.
- [11] J.D. Livingston, *Phys. Status Solidi A*, **70** (2), 591 (1982).  
DOI: 10.1002/pssa.2210700228